Thermal stress analysis of dry-type transformers under short-circuit conditions considering temperature-dependent epoxy properties

Pham Hong Hai*, Nguyen Trung Son, Le Duc Tung, Tran Anh Minh

School of Electrical and Electronic Engineering, Hanoi University of Science and Technology, 1 Dai Co Viet, Bach Mai, Hanoi, Vietnam.

*Corresponding author: hai.phamhong@hust.edu.vn

Received 27 Mar. 2026; Revised 17 May 2026; Accepted 10 Aug. 2026; Published 25 Aug. 2026.

DOI: https://doi.org/10.54939/1859-1043.j.mst.113.2026.20-29

ABSTRACT

Accurate prediction of temperature rise and hotspot formation is critical for the lifetime and safety of cast-resin dry-type transformers. Conventional thermal design methods typically assume constant thermophysical properties for epoxy insulation, neglecting their nonlinear temperature dependence - an oversimplification that can introduce significant errors under severe operating conditions such as short-circuit faults. This study applies a temperature-dependent thermal modeling approach to a 320 kVA, 22/0.4 kV amorphous-core dry-type transformer, employing coupled Finite Element Method (FEM) and Computational Fluid Dynamics (CFD) to simulate the three-dimensional transient temperature field with temperature-dependent thermal conductivity, diffusivity, and specific heat capacity of epoxy insulation. Results show that the high-voltage winding is the most thermally critical region under short-circuit conditions, and that incorporating temperature-dependent material properties yields higher predicted hotspot temperatures and stronger thermal stress concentration compared to conventional constant-property assumptions. These findings highlight the importance of temperature-dependent modeling in transformer thermal design and provide a more reliable basis for structural optimization and safety assessment.

Keywords: Dry-type transformer; Amorphous core; Temperature-dependent properties; Thermo-mechanical stress.

1. INTRODUCTION

Cast-resin dry-type transformers with amorphous cores are increasingly adopted in modern power distribution systems due to their high fire safety, environmental friendliness, and low no-load losses [1-2]. Despite these advantages, their structural reliability is strongly influenced by thermo-mechanical stresses arising from non-uniform temperature fields, particularly under overload and short-circuit conditions [3-7]. During such transient events, rapid temperature rises and steep thermal gradients develop within the windings and epoxy insulation. Due to the mismatch in thermal expansion coefficients between copper conductors and epoxy encapsulation, significant internal stresses may arise, potentially leading to insulation cracking, mechanical deformation, and long-term degradation [8, 9].

Numerous studies have employed finite-element-based and coupled multiphysics approaches to investigate the thermal and mechanical behavior of dry-type transformers[10,11]. While these studies have provided important insights into temperature distribution, hotspot formation, and stress evolution, most existing models assume constant thermophysical properties for epoxy insulation, including thermal conductivity, specific heat capacity, and thermal diffusivity [12-15]. Such assumptions neglect the pronounced nonlinear temperature dependence of epoxy properties, particularly at elevated temperatures, and may lead to inaccurate thermal predictions and unreliable thermo-mechanical assessments.

Experimental and numerical investigations have shown that the thermophysical properties of epoxy insulation vary significantly with temperature [16, 17]. Ignoring this behavior can result in underestimation of hotspot temperatures and thermal stresses, especially under short-circuit conditions characterized by high current surges and rapid heat generation. Therefore, incorporating temperature-dependent material properties into thermal modeling is essential for improving prediction accuracy and ensuring reliable transformer design.

In this study, a three-dimensional coupled FEM–CFD framework is proposed that explicitly incorporates temperature-dependent thermophysical properties of epoxy insulation. The model is applied to a 320 kVA, 22/0.4 kV cast-resin dry-type transformer to investigate its thermal and thermo-mechanical behavior under short-circuit conditions. By enhancing the fidelity of thermal analysis, the proposed approach enables more accurate identification of critical regions susceptible to excessive temperature rise and stress concentration, thereby providing a robust basis for structural optimization and operational safety assessment.

The main contributions of this work are as follows:

• Establishment of a fully coupled three-dimensional FEM–CFD framework for electromagnetic, thermal, and mechanical analysis under short-circuit conditions.

• Improved prediction of temperature distribution and thermo-mechanical stresses, enabling reliable identification of structurally critical regions.

The remainder of this paper is organized as follows. Section II presents the physical principles and numerical methodology. Section III discusses the simulation results, and Section IV concludes the paper.

2. RESEARCH METHODOLOGY

2.1. Physical theory

To analyze the thermal behavior and associated stresses of the dry-type transformer under short-circuit conditions, a coupled multiphysics framework integrating electromagnetic, thermal, and mechanical fields is adopted. The interaction among these physical domains is essential for accurately capturing heat generation, temperature evolution, and thermo-mechanical stress development during transient fault conditions.

2.1.1. Electromagnetic field model

The electromagnetic behavior of the transformer is governed by Maxwell's equations, including Gauss's laws for electric and magnetic fields, Faraday's law of induction, and the Ampère–Maxwell law.

Gauss's law for electric fields:

$$\nabla \cdot E = \frac{\rho_e}{\varepsilon_0} \tag{1}$$

Gauss's law for magnetism:

$$\nabla \cdot B = 0 \tag{2}$$

Faraday's law of induction:

$$\nabla \times E = -\frac{\partial B}{\partial t} \tag{3}$$

Ampère–Maxwell law:

$$\nabla \times B = \mu J + \mu \frac{\partial D}{\partial t} \tag{4}$$

Under the quasi-static operating conditions of interest, the displacement current can be neglected: $\frac{\partial D}{\partial t} \approx 0$

During a short-circuit event, the winding current may rise to several tens of times the rated current. The transient current consists of a steady-state periodic component and an exponentially decaying aperiodic component [11], and can be expressed as:

$$i = \sqrt{2}I_n\left[\sin(\omega t - \psi - \varphi_n) + \sin(\psi_n)\ e^{-\frac{R_n}{X_n}\omega t}\right] \tag{5}$$

Where: I_n is steady-state short-circuit current, R_n is the winding resistance, X_n is the short-circuit reactance, ψ is the switching angle at the instant of fault occurrence, φ_n is the phase angle. The resulting electromagnetic losses serve as the primary heat sources in the thermal analysis.

2.1.2. Thermal Field Model:

The thermal behavior of the transformer is mainly driven by electromagnetic losses, with winding losses dominating during short-circuit conditions due to the quadratic dependence on current magnitude.

Winding losses

Alternating current in the windings produces both fundamental and additional losses, which can be expressed by:

$$\Delta P_u = k_1 m_1 I_1^2 R_{1d} + k_2 m_2 I_2^2 R_{2d} \tag{6}$$

Where: I_1, I_2 are RMS currents of primary and secondary windings, R_{1d}, R_{2d} are DC phase resistances, k is an additional loss coefficient

Under overload or short-circuit conditions, the current increases significantly, resulting in a aquadratic increase in heat generation.

Core losses

Core losses consist of hysteresis loss and eddy current (Foucault) loss, which are generally expressed as:

Hysteresis loss

$$P_h = \eta f B^n \tag{7}$$

Eddy-current loss

$$P_w = \frac{4}{3}\frac{1}{\rho}\left(\frac{d}{2}\right)^2 f^2 B^2 \tag{8}$$

Heat Transfer Mechanisms:

The heat generated within the transformer is dissipated through three main mechanisms: conduction, convection, and radiation.

- Heat conduction within solid materials is governed by theFourier–Kirchhoff heat conduction equation:

$$\frac{\partial T}{\partial \tau} = \frac{\lambda}{C_\rho}\left(\frac{\partial^2 T}{\partial x^2} + \frac{\partial^2 T}{\partial y^2} + \frac{\partial^2 T}{\partial z^2}\right) + \frac{q_v}{C_\rho} \tag{9}$$

Where: T is the temperature (K), τ is time (s), λ is thermal conductivity (W/m·K), C_ρ is volumetric heat capacity (J/m³·K), q_v is volumetric heat source (W/m³)

- Given the extremely short duration of the fault (3 seconds), the thermal response of the windings is predominantly an adiabatic heating process. While convective and radiative boundaries are defined in the model for completeness, natural convection has a negligible effect within this brief timeframe. The generated heat cannot be dissipated into the surrounding air and is almost entirely accumulated locally, creating steep thermal gradients between the rapidly heating copper windings and the cooler, restraining epoxy insulation.

To solve the complex 3D thermo-mechanical problem, a sequential one-way multiphysics coupling strategy is implemented within the ANSYS Workbench environment. The analytical laws presented above represent the governing physics inherent within the software solvers. The overall workflow consists of three main steps:

1. Electromagnetic Analysis (ANSYS Maxwell): Computes the transient short-circuit current, volumetric heat generation rates (losses), and electromagnetic Lorentz forces.

2. Transient Thermal Analysis (ANSYS Fluent/Thermal): Imports the computed electromagnetic losses as volumetric heat sources to simulate the rapid 3-second temperature rise. Crucially, the solver continuously updates the temperature-dependent thermophysical properties of the epoxy based on the localized real-time temperature.

3. Static Structural Analysis: Imports both the spatial temperature distribution (to compute thermal expansion) and the electromagnetic forces to calculate the combined 3D thermo-mechanical stress tensor.

2.2. Mathematical model

A comprehensive numerical model is established to solve the coupled electromagnetic, thermal-fluid, and mechanical problems using the Finite Element Method (FEM) and Computational Fluid Dynamics (CFD).

2.2.1. Geometry and mesh generation

The 3D model of the 320 kVA, 22/0.4 kV dry-type transformer, shown in Figure 1, is constructed from the manufacturer's specifications. The model includes the amorphous core, the low-voltage winding, the high-voltage winding, and the epoxy insulation layers.

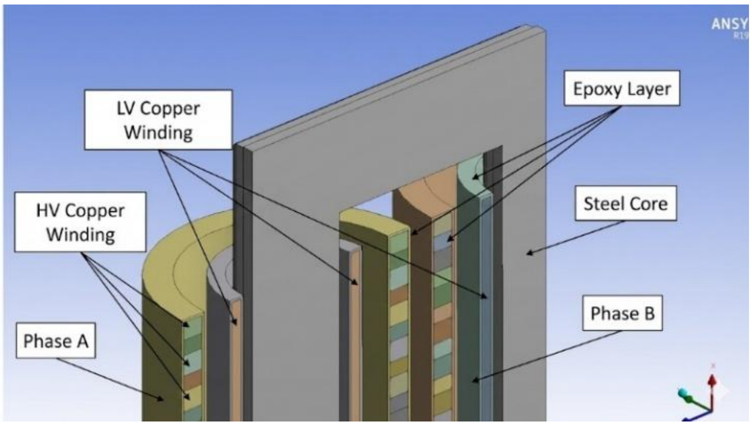

Figure 1. *3D model of the 320 kVA, 22/0.4 kV dry-type transformer.*

To achieve high simulation accuracy, especially at material interfaces, the computational domain is discretized using a high-quality hexahedral mesh.

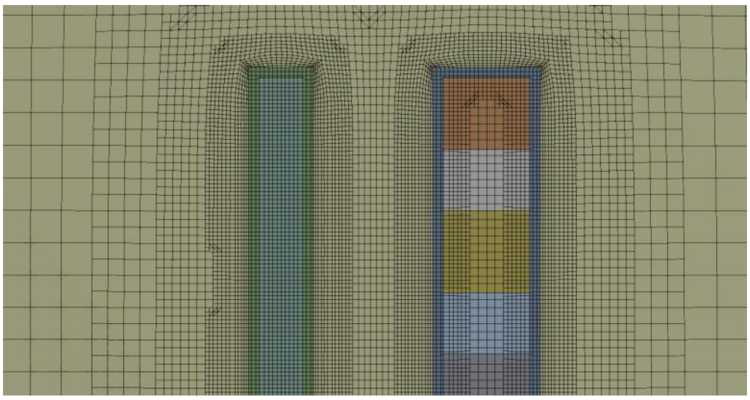

Figure 2. *Computational mesh used for transformer simulation.*

To eliminate grid-induced numerical errors, a rigorous mesh independence study was conducted. The grid was systematically refined from approximately 10 million to over 20 million elements. The comparative results confirmed that increasing the mesh count beyond 15.6 million elements resulted in a maximum hotspot temperature and peak stress deviation of less than 0.1%. Consequently, the grid with 15.6 million elements was definitively selected for all subsequent analyses, ensuring strict grid convergence while optimizing computational efficiency (Figure2).

2.2.2. Transformer parameters used in the simulation

The simulation parameters are based on the technical specifications of a 320 kVA, 22/0.4 kV dry-type transformer manufactured by SANAKY in Table 1.

Table 1. *Rated specifications of 320 kVA dry-typer transformer.*

Parameter	Value	Unit
Number of phases	3	-
Frequency	50	Hz
Rated power	320	kVA
Vector group	Δ/Yn11	-
HV/LV line voltage	22/0.4	kV
HV/LV phase turns W_1/W_2	2090/22	Turns
HV/LV line current	8.42/462	A
Short-circuit impedance u_k	6	%

The temperature-dependent properties of the epoxy insulation used in the model were adopted from the authors' previous studies [17, 18]. The following empirical relations were used in the present analysis:

Thermal conductivity:

$$\lambda(T) = 0.5612 + 2.044 \times 10^{-3}T - 1.68 \times 10^{-5}T^2 \quad (10)$$

Specific heat capacity:

$$c_p(T) = 82.61 + 4.77T + 0.031T^2 \quad (11)$$

Thermal diffusivity:

$$\alpha(T) = 2.33 - 0.031T + 21.05 \times 10^{-5}T^2 \quad (12)$$

3. SIMULATION RESULTS AND DISCUSSION

3.1. Baseline model validation under rated load

Before simulating the extreme short-circuit transient, the baseline 3D multiphysics model was rigorously validated under steady-state rated load conditions to ensure its computational fidelity. As extensively detailed in our foundational experimental research [19], the simulated temperature distribution was quantitatively compared against empirical data obtained from 27 discrete Type-T thermocouples installed directly on the actual 320 kVA dry-type transformer prototype. The validation results demonstrated a high degree of agreement; the baseline model integrating temperature-dependent epoxy properties maintained a maximum relative error of strictly less than 4.59% across all measuring points, significantly outperforming conventional constant-property models (which exhibited error margins up to ~10.9%). This strict baseline empirical validation confirms that the proposed multi-physics framework accurately replicates the complex heat transfer phenomena, thereby providing a highly reliable and robust foundation for extrapolating the model to compute the extreme thermal and mechanical responses during the 3-second short-circuit event.

3.2. Temperature distribution under short-circuit conditions

The transient temperature distribution under short-circuit conditions was simulated while the transformer operated at rated load. The total simulation time was 3 s with a time step of 0.01 s. For thermal analysis, a mesh containing approximately 15.6 million elements was used to ensure numerical convergence (Figure 3).

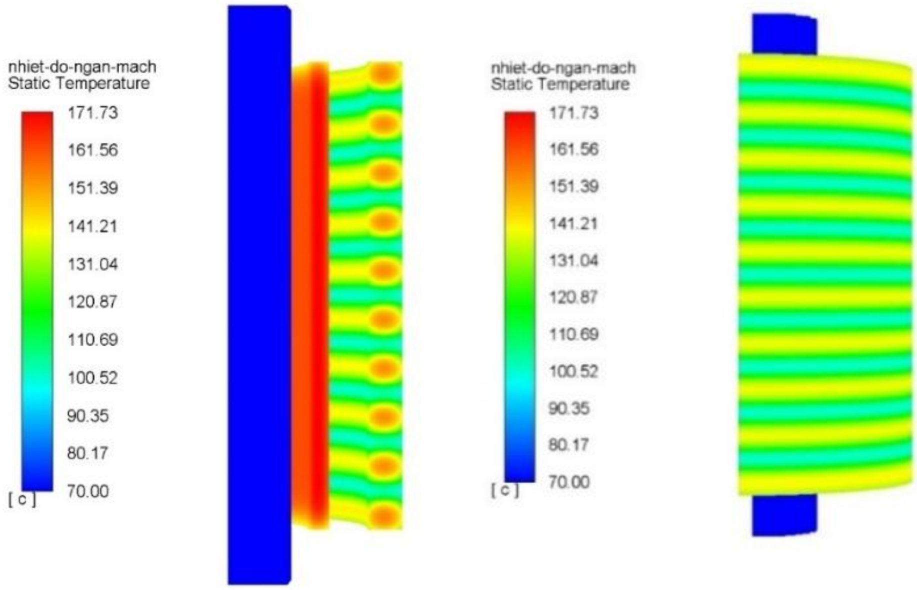

Figure 3. *Temperature distribution of the 320 kVA transformer under secondary short-circuit conditions after 3 s.*

Under short-circuit conditions, the highest temperature occurs in phase B and is primarily concentrated in the HV winding. The maximum HV winding temperature reaches 171.73 °C. The transient temperature rise of the LV and HV windings is presented in Figure 4.

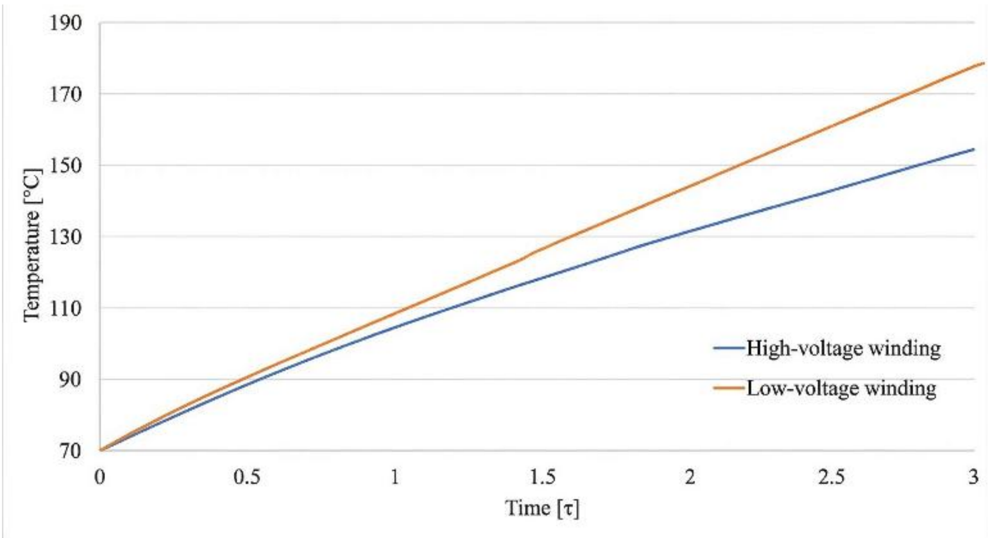

Figure 4. *Temperature rise of the low-voltage (LV) and high-voltage (HV) windings under short-circuit fault conditions.*

3.3. Thermal stress in the 320 kVA transformer under short-circuit conditions

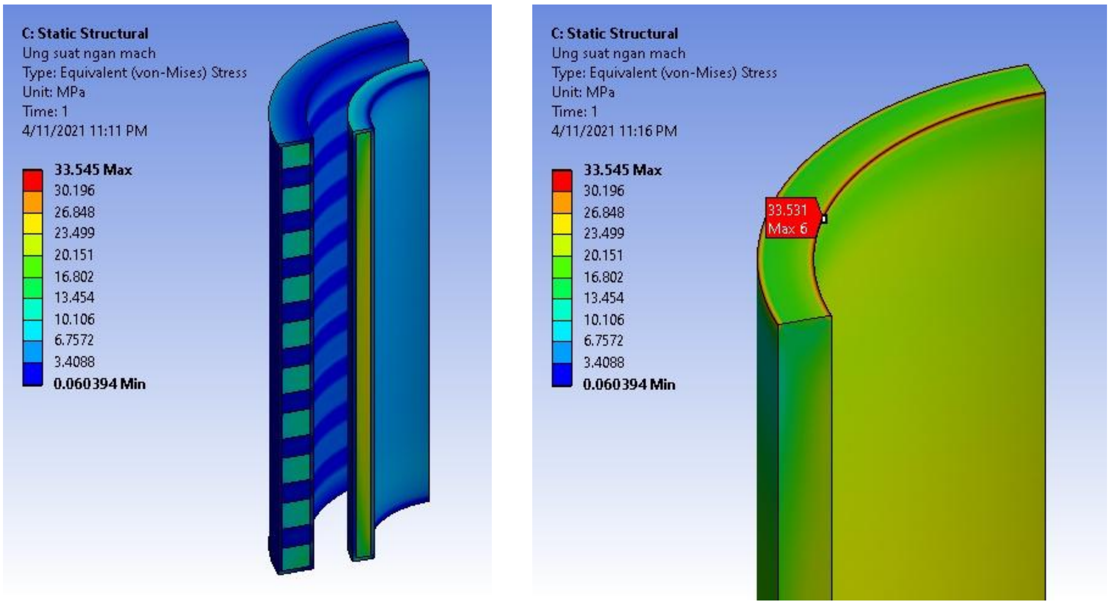

(a) (b)

Figure 5. *Distribution of thermal stress in (a) the LV and HV windings of phase B and (b) the region of maximum stress in the phase B HV winding.*

After 3 s of short-circuit operation, the average thermal stress in the transformer reaches 8.256 MPa (Figure 6). The maximum thermal stress occurs at the upper corner of the phase B HV winding, where it reaches 33.5 MPa (Figure7).

Tabular Data

	Time [s]	Minimum [MPa]	Maximum [MPa]	Average [MPa]
1	1.	6.0394e-002	33.545	8.256

Figure 6 *Thermal stress distribution in the transformer after 3 s short-circuit.*

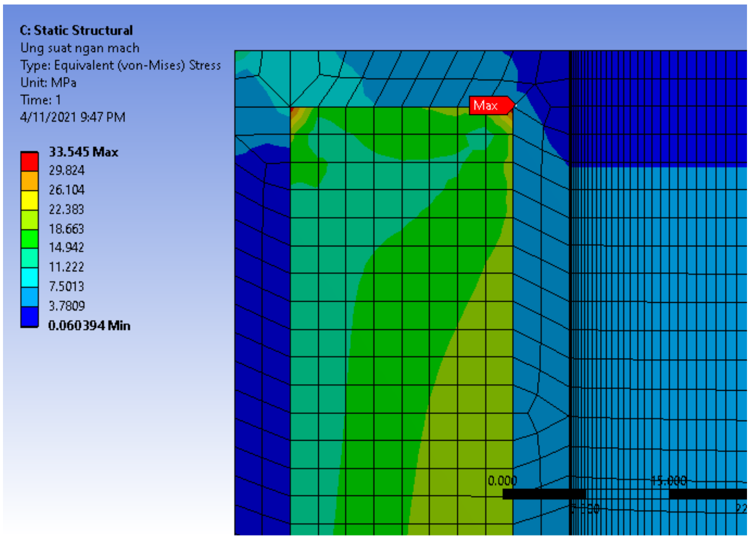

Figure 7. *Location of the peak thermal stress at the upper corner of the phase B high-voltage winding.*

3.4. Combined short-circuit stress in the 320 kVA transformer

The stress acting on the windings of the epoxy-insulated dry-type transformer is the result of electromagnetic forces, thermal stress caused by the temperature difference between the windings and the epoxy insulation, and the stress generated bythe non-uniform temperature distribution within the epoxy layer.

After the electromagnetic force stress and the thermal stress are determined, the combined stress at each winding location can be evaluated (Figure 8).

The maximum combined short-circuit stress in the HV winding is $\sigma_{\Sigma,HV} = 85.462$MPa, occurring at the middle of the HV winding along the axial direction y.

The maximum combined short-circuit stress in the LV winding is $\sigma_{\Sigma,LV} = 65.77$MPa, occurring at the middle of the LV winding along the axial direction y.

These values remain lower than the allowable stresses of copper $[\sigma_{Cu}] = 120$MPa and epoxy $[\sigma_{epoxy}] = 100$MPa

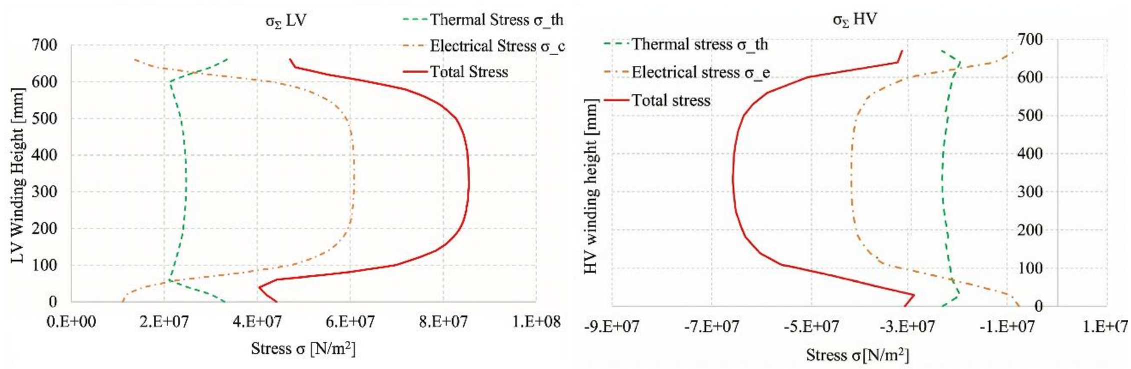

(a) *(b)*

***Figure 8.** Combined short-circuit stress distribution on the transformer windings: (a) Outer edge of the LV winding; (b) Innermost edge of the HV winding.*

The results also show that the electromagnetic forces produces high stresses in the boundary regions near the ends of the HV winding. During short-circuit events, these stresses are further amplified by thermal stress, because the stresses generated in the epoxy insulation act in the same direction as the electromagnetic stress. Therefore, appropriate structural reinforcement and manufacturing measures are required to mitigate the mechanical risk in these critical regions.

4. CONCLUSIONS

This study developed a three-dimensional multiphysics model for a 320 kVA, 22/0.4 kV amorphous-core dry-type transformer by coupling FEM and CFD analyses and incorporating experimentally determined temperature-dependent thermophysical properties of epoxy insulation. Compared with conventional thermal models that assume constant material properties, the proposed approach provides a more realistic representation of heat transfer within the transformer and offers a stronger basis for predicting hotspot formation and thermal loading under severe operating conditions.

The simulation results indicate that the high-voltage winding is the most critical region under short-circuit conditions, where both temperature concentration and maximum stress are most likely to occur. The coupled thermo-mechanical analysis further reveals that short-circuit events generate significant combined stresses within the winding structure, particularly near the winding ends and other boundary regions. Although the computed stresses remain below the allowable limits of copper conductors and epoxy insulation materials, these regions require special attention during design and manufacturing to ensure structural integrity and operational reliability.

Overall, the proposed temperature-dependent thermal model provides a more reliable tool for evaluating transformer thermal performance, assessing insulation durability, and supporting the design optimization of dry-type transformers operating under overload and short-circuit conditions. The outcomes of this study can serve as a valuable reference for improving safety margins and mechanical robustness in cast-resin dry-type transformer designs.

REFERENCES

[1]. Bonneville Power Administration, *"Dry-type transformer new construction and retrofit energy savings potential,"* BPA, (2021).

[2]. P. Kumar and P. Verma, *"Review paper on diagnostics study of dry transformer,"* CEUR Workshop Proc., vol. 3058, pp. 1–3, (2021).

[3]. B. Doan Thanh, *"Determination of winding destroy limit area for a power series of amorphous core transformers,"* J. Mil. Sci. Technol., vol. 103, no. 103, pp. 11–21, (2025). DOI: 10.54939/1859-1043.j.mst.103.2025.11-21

[4]. D. S. He et al., *"Simulation and experimental analysis of dynamic thermal rise relaxation characteristics for dry-type distribution transformer,"* Int. J. Emerging Electric Power Syst., vol. 26, no. 2, pp. 419–435, (2025). DOI: 10.1515/ijeeps-2024-0106

[5]. Z. Guan et al., *"Research on the thermal aging characteristics of epoxy resin for high frequency transformers based on activation energy,"* in Proc. IEEE Int. Conf. Electrical Materials and Power Equipment (ICEMPE), Harbin, China, pp. 1–5, (2025). DOI: 10.1109/ICEMPE66159.2025.11122976

[6]. B. D. Thanh, T. H. Le, and V. D. Quoc, *"A comparative analysis of axial and radial forces in windings of amorphous core transformers,"* Int. J. Electr. Eng. Educ., (2024). DOI: 10.5829/ije.2024.37.01a.18

[7]. B. D. Thanh, D. D. Tung, and T.-H. Le, *"Computation of electromagnetic forces in the windings of amorphous core transformers,"* Arch. Electr. Eng., (2023). DOI: 10.24425/aee.2023.145423

[8]. Y. Sun et al., *"Hotspot temperature prediction of dry-type transformers based on particle filter optimization with support vector regression,"* Symmetry, vol. 13, no. 8, p. 1320, (2021). DOI: 10.3390/sym13081308

[9]. Y. Wang, C. Feng, R. Fei, and Y. Luo, *"Thermal-ageing characteristics of dry-type transformer epoxy composite insulation,"* High Performance Polym., vol. 32, no. 7, pp. 741–752, (2020). DOI: 10.1177/0954008320906439

[10]. B. T. Doan, *"Calculation of temperature distribution of air-cooled three-phase dry transformer,"* J. Sci. Technol. – Univ. Danang, vol. 20, no. 11.2, pp. 38–43, (2022).

[11]. P. H. Hai et al., *"Calculation of electromagnetic force and temperature distribution of amorphous transformers in different operating modes by finite element method,"* CTU J. Innovation Sustainable Dev., vol. 16, no. 1, pp. 66–75, (2024). DOI: 10.22144/ctujsd.2024.269

[12]. K. Dawood and S. Kul, *"Influence of core window height on thermal characteristics of dry-type transformers,"* Case Stud. Therm. Eng., (2025). DOI: 10.1016/j.csite.2025.105746

[13]. M. S. Seddik, J. Shazly, and M. B. Eteiba, *"Thermal analysis of power transformer using 2D and 3D finite element method,"* Energies, vol. 17, no. 13, p. 3203, (2024). DOI: 10.3390/en17133203

[14]. J. P. Américo, J. V. Leite, and C. F. Mazzola, *"Enhanced thermal modeling of three-phase dry-type transformers,"* Case Stud. Therm. Eng., vol. 58, p. 104445, (2024). DOI: 10.1016/j.csite.2024.104445

[15]. D. S. He, Z. D. Jia, J. X. Wang, J. B. Fu, F. He, and F. Dai, *"Investigating temperature rise dynamics at hot-spots within dry-type transformer windings: A comparative analysis across varied loading rates and an extrapolative computational model,"* Case Stud. Therm. Eng., vol. 60, p. 104699, (2024). DOI: 10.1016/j.csite.2024.104699

[16]. M. De Melo Antunes et al., *"Estimation of effective temperature-dependent thermal properties of glass fiber-reinforced polymer for air-core reactor insulation: A case study using an alternative inverse approach,"* Int. J. Thermophysics, vol. 45, no. 12, (2024). DOI: 10.1007/s10765-024-03468-3

[17]. P. H. Hai et al., *"A study on thermal properties of epoxy materials in a dry-type transformer,"* J. Sci. Technol. – Univ. Danang, vol. 19, no. 7, pp. 29–34, (2021).

[18]. P. H. Hai and L. D. Tung, *"Study on the thermal distribution of dry-type transformer with epoxy-cast windings at rated load and partial load,"* J. Meas., Control Autom., vol. 28, no. 3, pp. 47–52, (2024).

[19]. H. H. Pham, *"Nghiên cứu lực ngắn mạch tổng hợp có tính đến ảnh hưởng phân bố nhiệt trong máy biến áp khô có lõi thép vô định hình,"* Thesis, Hanoi University of Science and Technology, Hanoi, Vietnam, (2021) (in Vietnamese).

TÓM TẮT

Phân tích ứng suất nhiệt máy biến áp khô trong sự cố ngắn mạch sử dụng các thông số epoxy phụ thuộc nhiệt độ

Dự đoán chính xác sự tăng nhiệt độ và hình thành điểm nóng là rất quan trọng đối với tuổi thọ và sự an toàn của máy biến áp khô lõi nhựa đúc. Các phương pháp thiết kế nhiệt thông thường thường giả định các tính chất nhiệt vật lý không đổi của vật liệu cách điện epoxy, bỏ qua sự phụ thuộc phi tuyến tính của chúng vào nhiệt độ - một sự đơn giản hóa quá mức có thể gây ra sai sót đáng kể trong điều kiện hoạt động khắc nghiệt như sự cố ngắn mạch. Nghiên cứu này áp dụng phương pháp mô hình hóa nhiệt phụ thuộc vào nhiệt độ cho máy biến áp khô lõi vô định hình 320 kVA, 22/0,4 kV, sử dụng phương pháp phần tử hữu hạn (FEM) và động lực học chất lỏng tính toán (CFD) kết hợp để mô phỏng trường nhiệt độ tức thời ba chiều với độ dẫn nhiệt, độ khuếch tán nhiệt và nhiệt dung riêng phụ thuộc vào nhiệt độ của vật liệu cách điện epoxy. Kết quả cho thấy cuộn dây cao áp là vùng quan trọng nhất về mặt nhiệt trong điều kiện ngắn mạch, và việc kết hợp các tính chất vật liệu phụ thuộc vào nhiệt độ dẫn đến nhiệt độ điểm nóng dự đoán cao hơn và sự tập trung ứng suất nhiệt mạnh hơn so với các giả định tính chất không đổi thông thường. Những phát hiện này nhấn mạnh tầm quan trọng của mô hình hóa phụ thuộc vào nhiệt độ trong thiết kế nhiệt máy biến áp và cung cấp cơ sở đáng tin cậy hơn cho việc tối ưu hóa cấu trúc và đánh giá an toàn.

Từ khoá: Máy biến áp khô; Lõi vô định hình; Đặc tính phụ thuộc nhiệt độ; Ứng suất nhiệt – cơ học.